NEOPLASIA
www.neoplasia.com

Volume 14 Number 8 August 2012 pp. 670–677 670

Wild-type EGFR Is Stabilized by Direct Interaction with HSP90 in Cancer Cells and Tumors[1,2]

Aarif Ahsan*, Susmita G. Ramanand*, Christopher Whitehead†, Susan M. Hiniker*, Alnawaz Rehemtulla*, William B. Pratt‡, Shruti Jolly*, Christopher Gouveia§, Kristy Truong§, Carter Van Waes§, Dipankar Ray*, Theodore S. Lawrence* and Mukesh K. Nyati*

*Department of Radiation Oncology, University of Michigan, Ann Arbor, MI; †Department of Radiology, University of Michigan, Ann Arbor, MI; ‡Department of Pharmacology, University of Michigan, Ann Arbor, MI; §Head and Neck Surgery Branch, National Institute on Deafness and Other Communication Disorders, National Institutes of Health, Bethesda, MD

Abstract

The epidermal growth factor receptor (EGFR) has been targeted for inhibition using tyrosine kinase inhibitors and monoclonal antibodies, with improvement in outcome in subsets of patients with head and neck, lung, and colorectal carcinomas. We have previously found that EGFR stability plays a key role in cell survival after chemotherapy and radiotherapy. Heat shock protein 90 (HSP90) is known to stabilize mutant EGFR and ErbB2, but its role in cancers with wild-type (WT) WT-EGFR is unclear. In this report, we demonstrate that fully mature, membrane-bound WT-EGFR interacts with HSP90 independent of ErbB2. Further, the HSP90 inhibitors geldanamycin (GA) and AT13387 cause a decrease in WT-EGFR in cultured head and neck cancer cells. This decrease results from a significantly reduced half-life of WT-EGFR. WT-EGFR was also lost in head and neck xenograft specimens after treatment with AT13387 under conditions that inhibited tumor growth and prolonged survival of the mice. Our findings demonstrate that WT-EGFR is a client protein of HSP90 and that their interaction is critical for maintaining both the stability of the receptor as well as the growth of EGFR-dependent cancers. Furthermore, these findings support the search for specific agents that disrupt HSP90's ability to act as an EGFR chaperone.

Neoplasia (2012) 14, 670–677

Introduction

Several common epithelial cancers are driven by epidermal growth factor receptor (EGFR)–mediated signaling. In the past decade, numerous agents that inhibit EGFR activity have been developed and been the subjects of rigorous preclinical and clinical studies. Recent studies have suggested that therapy-induced degradation of EGFR, not its inhibition, may correlate better with clinical outcome [1–9]. Although ligand-induced, ubiquitin-mediated changes in EGFR trafficking and degradation have been well studied in normal cells [10–12], little is known about how EGFR protein stability is regulated in tumor cells. We believe that a precise understanding of the regulation of EGFR protein stability will be useful in developing new classes of therapeutic agents that can promote tumor-specific degradation of EGFR independent of its kinase activity.

Abbreviations: CHX, cycloheximide; GA, geldanamycin; EGFR, epidermal growth factor receptor; HSP90, heat shock protein 90; WT, wild-type

Address all correspondence to: Mukesh K. Nyati, PhD, Department of Radiation Oncology, University of Michigan, Ann Arbor, MI 48109. E-mail: nyati@umich.edu

[1]This work was supported by R01CA131290, P50 CADE97248, Michigan Institute for Clinical and Health Research, University of Michigan Cancer Center support grant 5 P30 CA46592, and the James Stuart and Barbara Padnos Research Funds for Cancer Research (M.K. Nyati), NIDCD intramural program project ZIA-DC-000073 (C. Van Waes), and an Alfred Taubman Scholarship (T.S. Lawrence).

[2]This article refers to supplementary materials, which are designated by Figures W1 and W2 and are available online at www.neoplasia.com.

Received 20 June 2012; Revised 28 June 2012; Accepted 28 June 2012

DOI 10.1593/neo.12986

Heat shock protein 90 (HSP90) is a molecular chaperone that is known to regulate stability of various oncogenic kinases [13,14], especially under proteotoxic stress. HSP90 has been implicated in the stability of ErbB2 and tyrosine kinase inhibitor (TKI)–resistant (*T790M EGFR*), –truncated (*EGFRvIII*), or –nascent EGFR [15–17]. Whereas nascent and mutated EGFR have been shown to be HSP90 clients, conclusive evidence is still lacking regarding whether mature, wild-type (WT) EGFR is an HSP90 client, particularly under conditions in which EGFR is overexpressed.

We hypothesized that, in head and neck cancers where WT-EGFR is often overexpressed, HSP90 interaction promotes receptor stability and cell survival. Therefore, we carried out experiments to determine whether mature plasma membrane–bound WT-EGFR binds to HSP90 and to assess whether this interaction was direct or was mediated by ErbB2. When we found a direct interaction between mature EGFR and HSP90, we determined how inhibition of HSP90 activity affected the half-life of WT-EGFR. We then assessed the effect of HSP90 inhibition by AT13387 on EGFR stability and tumor growth in UMSCC1 head and neck xenografts. Our findings support clinical investigation of HSP90 inhibitors in cancers overexpressing WT as well as mutant EGFR and motivate studies to identify site(s) by which EGFR and HSP90 interact as a specific way to promote EGFR degradation and decrease cancer cell survival.

Materials and Methods

Reagents

AT13387 compound was provided by Astex Pharmaceuticals (Cambridge, United Kingdom) through a Materials Transfer Agreement with the National Cancer Institute (NCI, Bethesda, MD). Geldanamycin (GA) was acquired from Assay Designs (Ann Arbor, MI). EGFR (sc-03) antibody was acquired from Santa Cruz Biotechnology (Santa Cruz, CA). Antibodies for EGFR (D38B1), ErbB2, GAPDH, HSP70, and cleaved poly (ADP-ribose) polymerase were purchased from Cell Signaling (Danvers, MA), whereas antibodies to detect ErbB2 were purchased from Neomarkers (Kalamazoo, MI). Another EGFR antibody (31G7) was purchased from Invitrogen (Grand Island, NY). Antibody against HSP90 was purchased from Pharmingen (San Diego, CA). Cycloheximide (CHX) and FLAG (M2) antibody were obtained from Sigma-Aldrich (St Louis, MO). For immunofluorescence, HSP90 antibody from Enzo Life Sciences, Inc (Farmingdale, NY) was used. The FLAG-Tagged HSP90 construct was a gift from L. Neckers (NCI).

Cell Culture

The human head and neck squamous cell carcinoma (HNSCC) cell lines UMSCC1, 11B, 12, 17B, 29, 33, and 74B were kindly provided by Dr Thomas Carey (University of Michigan, Ann Arbor, MI). The lung cancer cell line NCI-H1975 was provided by J. Engelman (Massachusetts General Hospital, Boston, MA). BT474, SW620, and Chinese hamster ovary (CHO) cells were purchased from the American Type Culture Collection (Manassas, VA). All cell lines were grown in RPMI 1640 supplemented with 10% cosmic calf serum. For all *in vitro* experiments, cells were released from flasks using phosphate-buffered saline (PBS) containing 0.01% trypsin and 0.20 mM EDTA, and cells were plated onto culture dishes 2 days before treatment.

Immunoblot Analysis

Cells were scraped into PBS-containing sodium orthovanadate and protease inhibitor cocktail (Roche Diagnostic Co, Indianapolis, IN). Cells were incubated for 15 minutes on ice in Laemmli buffer (63 mM Tris-HCl, 2% [wt/vol] SDS, 10% [vol/vol] glycerol, and 0.005% [wt/vol] bromophenol blue) containing 100 mM NaF, 1 mM Na_3VO_4, 1 mM phenylmethylsulfonyl fluoride, and 1 μg/ml aprotinin. After sonication, cell lysates were clarified by centrifugation at 13,000 rpm for 5 minutes at 4°C. The soluble protein fraction was heated to 95°C for 5 minutes, applied to a 4% to 12% bis-tris precast gel (Invitrogen), and transferred onto a polyvinylidene difluoride membrane. Membranes were incubated for 1 hour at room temperature in blocking buffer consisting of 3% bovine serum albumin and 1% normal goat serum in Tris-buffered saline (137 mM NaCl, 20 mM Tris-HCl [pH 7.6], and 0.1% [vol/vol] Tween 20). Membranes were subsequently incubated overnight at 4°C with 1 μg/ml primary antibody in blocking buffer, washed, and incubated for 1 hour with horseradish peroxidase–conjugated secondary antibody (Cell Signaling). After three additional washes in Tris-buffered saline, the bound antibody was detected by enhanced chemiluminescence plus reagent (Amersham Biosciences, Piscataway, NJ). For quantification of relative protein levels, immunoblot films were scanned and analyzed using ImageJ 1.46m software (National Institutes of Health, Bethesda, MD). Unless otherwise indicated, the relative protein levels shown represent a comparison to untreated controls.

Immunoprecipitation

Cells were trypsinized, washed twice with PBS, and cell lysates were prepared by incubation for 30 minutes on ice in fresh lysis buffer (1% Triton X-100, 0.1% sodium dodecyl sulfate, 0.15 M sodium chloride, 0.01 M sodium phosphate, pH 7.2 1 mM phenylmethylsulfonyl fluoride, 2 μg/ml aprotinin, 0.2 mM sodium orthovanadate, 50 mM sodium fluoride, 2 mM EDTA, 20 mM ammonium molybdate). Immunoprecipitation of EGFR and HSP90 was performed as described previously [18]. For subcellular fractionation studies, cytosolic, nuclear, and membrane fractions were isolated using a Compartment Protein Extraction Kit (Millipore, Billerica, MA). The purity of fraction in the input was confirmed by immunoblot analysis with HSP90 (cytosol), EGFR (membrane), and poly (ADP-ribose) polymerase (nucleus). The extracts from these fractions were subjected to immunoprecipitation (IP), and the interaction between EGFR and HSP90 was assessed by immunoblot analysis.

Immunostaining

The Tissue and Histology Core of the Comprehensive Cancer Center and the Pathology Core for Animal Research in the Unit for Laboratory Animal Medicine at the University of Michigan provided assistance in preparing specimens for immunohistochemistry. After slides were deparaffinized in xylene and rehydrated using serial ethanol dilutions, antigen site unmasking was performed by immersing slides in citrate buffer for 20 minutes at high pressure and temperature inside a pressure cooker. Slides were then washed in PBS, blocked for 1 hour, and incubated in primary antibody at 4°C overnight. Slides were then washed again in PBS, incubated in secondary antibody for 1 hour, rewashed, and prepared with a coverslip after a drop of ProLong Gold antifade reagent with 4′,6-diamidino-2-phenylindole (Molecular Probes) was added to each sample. Fluorescence images were acquired using DS-Fi1 (Nikon, Melville, NY) camera fitted on an Olympus 1X-71 microscope. For costaining, cells were grown

on coverslips and fixed with paraformaldehyde. The coverslips were blocked and incubated with antibodies to EGFR and HSP90 overnight. The coverslips were processed as described above.

GST EGFR-HSP90 Direct Interaction Assay

Purified GST-EGFR (His672-Ala1210, 90 kDa, 1 μg) fusion protein (Cell Signaling) was incubated with 50 μl (3.5 mg swelled in deionized water) of glutathione agarose beads (Sigma-Aldrich) equilibrated in 0.5× Superdex buffer (1× Superdex buffer: 25 mM HEPES, pH 7.5, 12.5 mM $MgCl_2$, 10 μM $ZnSO_4$, 150 mM KCl, 20% glycerol, 0.1% Nonidet P-40, and 1 mM EDTA) for 2 hours at 4°C and then washed three times with 0.5× Superdex buffer. Two hundred nanograms of purified HSP90 protein (Assay Designs) was then added to the washed beads and incubated overnight at 4°C. The beads were washed three times using 0.5× Superdex buffer and boiled in Laemmli buffer, and the bound HSP90-EGFR complex was detected by immunoblot analysis with HSP90- and EGFR-specific antibodies.

Half-life Studies of EGFR

UMSCC1 cells were treated with vehicle or AT13387 (30 nM) for 12 hours followed by CHX (100 μg/ml). Cells were then harvested at different time points (0-15 hours). The effect of HSP90 inhibition

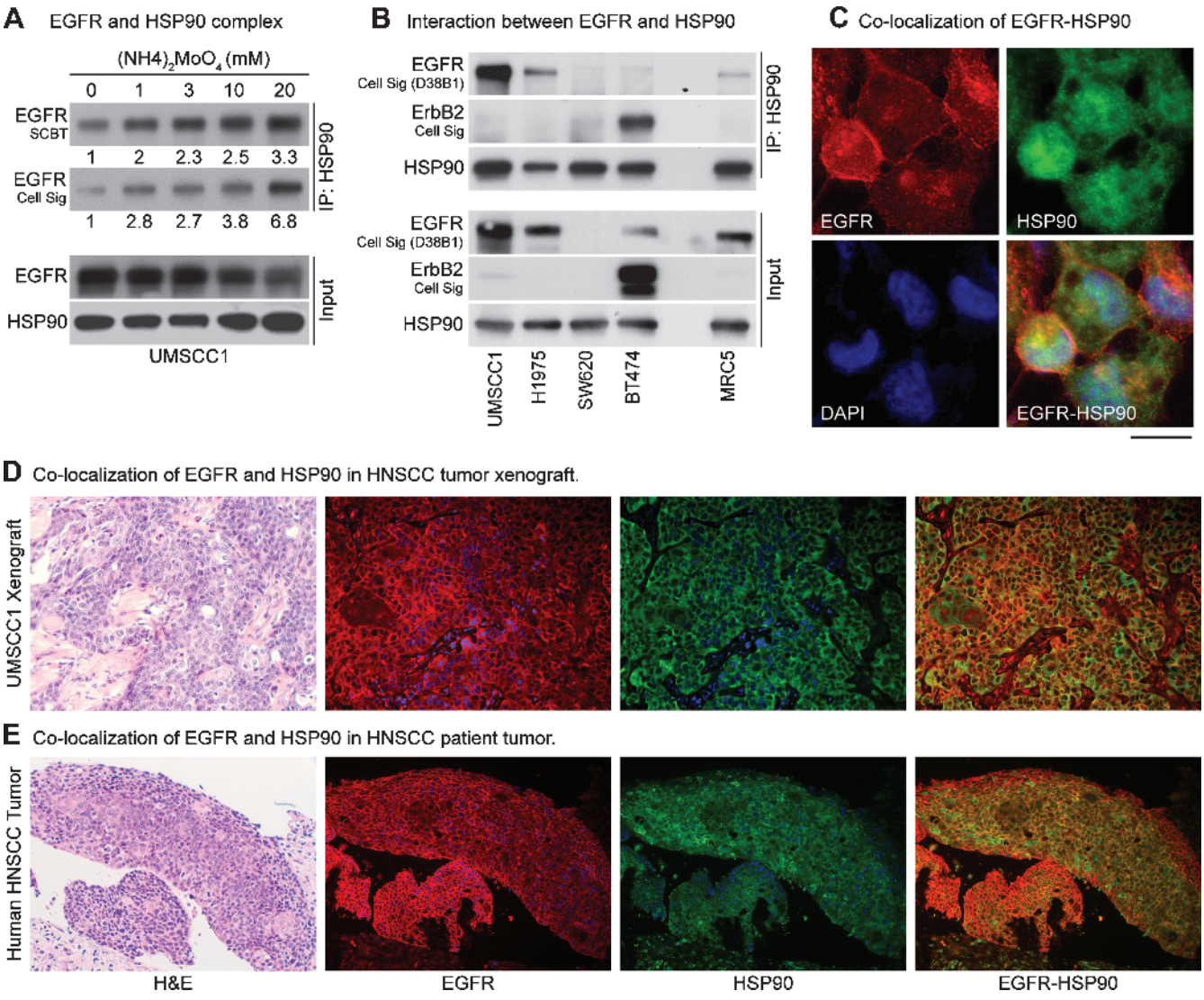

Figure 1. Interaction of WT-EGFR with HSP90. Immunoprecipitation using anti-HSP90 antibody revealed minimum EGFR in the complex; therefore, ammonium molybdate (20 mM), which is known to stabilize the interaction of HSP90 with its client proteins, was added to the lysis buffer. (A) IP results showed an increase in EGFR-HSP90 interaction with increasing concentrations of ammonium molybdate. Densitometric analysis of the films was performed using ImageJ software, and relative intensity is shown. Two EGFR antibodies were used to confirm these results. (B) Interaction between HSP90 and EGFR was assessed in five cell lines, representing normal EGFR-expressing cells (MRC5), EGFR-negative (SW620), ErbB2-driven, EGFR-independent (BT474), erlotinib-resistant (T790M-EGFR; NCI-H1975), and EGFR-amplified (UMSCC1) tumor cells. To address the issue of cross-reactivity, multiple EGFR antibodies were used, and their pattern was compared with ErbB2. One EGFR and one ErbB2 antibody were selected for the IP experiments. UMSCC1 and NCI-H1975 cell lines showed maximum interaction between EGFR with HSP90, whereas BT474 and MRC5 cells showed minimal interaction. EGFR-HSP90 interaction was absent in EGFR null SW620 cells. Colocalization of EGFR and HSP90 in tumor cells, xenografts, head and neck cancer patient's tumor was assessed by dual immunostaining for EGFR and HSP90. (C) UMSCC1 cells showed modest colocalization of these two proteins, which was also confirmed in (D) xenograft and (E) patient tumor specimen.

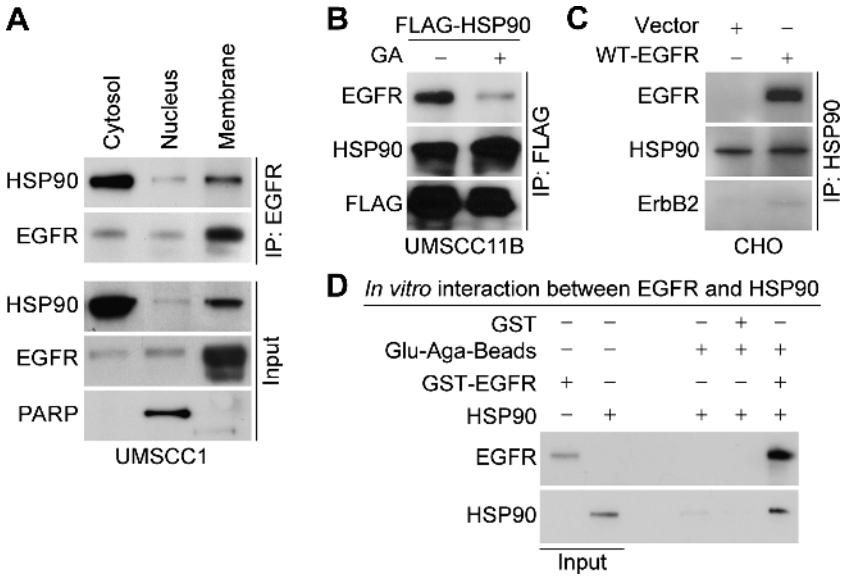

Figure 2. Localization, specificity, and nature of EGFR and HSP90 interaction. (A) To analyze whether the mature form of EGFR interacts with HSP90, subcellular fractionation followed by IP was carried out in UMSCC1 cells. EGFR-HSP90 interaction was confirmed in cytosolic, nuclear, and membrane fractions of UMSCC1 cells. (B) The specificity of this interaction was confirmed by expression of FLAG-tagged HSP90 in UMSCC11B cells, incubated with or without GA or (C) full-length EGFR in EGFR-negative CHO cells. (D) Direct interaction between EGFR and HSP90 was confirmed *in vitro* by GST pull-down assay.

on EGFR half-life was assessed using immunoblot analysis with the anti-EGFR antibody.

Animal Studies

Immunodeficient BALB/c SCID mice were injected subcutaneously on the right flank with 5×10^6 UMSCC1 cells. Once tumors were palpable, animals were randomized into treatment groups. AT13387 (55 mg/kg for two consecutive days; Monday and Tuesday weekly) suspended in cyclodextrin was administered through intraperitoneal injections [19,20]. Tumor size was measured three times per week, and tumor volumes were calculated as follows: volume (cm^3) = ($L \times W^2$) / 2. Two vehicle and three AT13387-treated mice were euthanized on day 16, tumors were harvested, and the effect of AT13387 on EGFR, ErbB2, and HSP70 was analyzed by immunoblot analysis.

Head and Neck Tumor Biopsy

The patient biopsy was obtained from a newly diagnosed pathology-proven locally advanced head and neck squamous cell carcinoma. At the time of this biopsy, the patient had not undergone any chemotherapy or radiation therapy. The tissue was fixed in formalin and processed for immunostaining.

Results

WT-EGFR Interacts with HSP90 in Cell Lines and Head and Neck Tumors

In our pilot experiments using standard conditions [21], we found that only a small amount of EGFR was immunoadsorbed by HSP90 antibody (Figure W1, *first lane*). We hypothesized that this could be due to the dynamic nature of EGFR-HSP90 interaction and that stabilization of this complex would increase the amount of EGFR that would be immunoadsorbed with HSP90. Therefore, we used ammonium molybdate, which is known to stabilize HSP90 clients [22], in the lysis buffer and found approximately a three-fold increase in immunoadsorbed full-length mature EGFR (Figures 1*A* and W1). We next determined the specificity of this interaction with HSP90 using multiple cell lines, chosen to represent various forms of EGFR or ErbB2, such as UMSCC1 (amplified EGFR), NCI-H1975 (erlotinib-resistant T790M-mutated EGFR), SW620 (EGFR null), BT474 (ErbB2-overexpressing, EGFR-independent), and normal lung fibroblast MRC5 (normal expression of WT-EGFR). We found a substantial interaction between EGFR and HSP90 in UMSCC1 and NCI-H1975 tumor cells, no interaction with SW620 (null) cells, and little interaction in MRC5 cells and BT474 cells (Figure 1*B*). We assessed the relative expression of EGFR and ErbB2 in these cell lines using several antibodies against EGFR to ensure that this interaction was not due to a cross-reactivity of EGFR antibodies to ErbB2. Next, we confirmed the specificity of interaction in six other HNSCC cell lines (UMSCC11B, 12, 17B, 29, 33, and 74B) by performing IP using not only HSP90 but also EGFR antibody (Figure W2). We extended the immunoadsorption studies further to assess if EGFR were colocalized with HSP90 in tumor cells, xenografts, and HNSCC patient tumors, which are known to overexpress EGFR. We observed modest costaining of HSP90 and EGFR in all the tissues (Figure 1, *C-E*). Overall, these data indicate that WT and fully mature EGFR do interact with HSP90 especially under conditions of EGFR overexpression and that the colocalization is only modest under less stressful (untreated) conditions, which suggests a potential role of HSP90 in WT-EGFR protein stability.

Mature EGFR Physically Interacts with HSP90

As the HSP90-bound EGFR had an apparent size of 170 kDa, which is the size of the membrane-bound mature form, we wished to determine whether the HSP90-EGFR interaction occurs in the cell membrane. For this analysis, subcellular cytosolic, nuclear, and membrane fractions were isolated from UMSCC1 cells, and EGFR-bound

HSP90 was resolved. We found that both cytosolic (nascent) and membrane-bound (mature) forms of EGFR interact with HSP90 (Figure 2*A*). The specificity of this interaction was further confirmed by expression of FLAG-tagged HSP90 in UMSCC11B cells followed by IP using anti-FLAG antibody (Figure 2*B*). HSP90 inhibition by GA reduced this interaction, indicating that HSP90 activity might be necessary for its interaction with EGFR.

Because both EGFR and HSP90 are known to interact directly with ErbB2 [23,24], we wished to rule out the possibility that the interaction between EGFR and HSP90 is through ErbB2. Therefore, we carried out experiments using CHO cells, which are both EGFR- and ErbB2-negative [6]. In this case, we were able to immunoprecipitate ectopically expressed WT-EGFR using anti-HSP90 antibody, suggesting that this interaction is not mediated by ErbB2 (Figure 2*C*). We also confirmed that this interaction was not mediated through Src or AKT (data not shown). To further assess if this interaction were direct, we performed *in vitro* GST pull-down assays using GST-EGFR and HSP90 protein. The complex was detected by immunoblot analysis suggestive of a direct interaction between EGFR and HSP90 (Figure 2*D*). Overall, these results show that the stability of oncogenic WT-EGFR may depend on its interaction with HSP90, that this interaction is direct and not mediated by heterodimerization of EGFR with ErbB2, and that the EGFR-HSP90 interaction is enhanced in tumor compared with normal cells.

HSP90 Inhibition Degrades WT-EGFR

The interaction of HSP90 with EGFR has been thought to be limited to nascent protein under conditions of normal EGFR expression [17,21]. To investigate the effect of HSP90 inhibition on mature WT-EGFR in cells overexpressing EGFR, we selected two head and neck cancer cell lines that express relatively similar amounts of ErbB2 (known to be an HSP90 client [25]) and WT-EGFR (UMSCC1 and UMSCC29) and assessed the effect of two HSP90 inhibitors (GA and AT13387) on EGFR protein levels relative to ErbB2. Both GA and AT13387 induced EGFR and ErbB2 degradation in a concentration-dependent manner (Figure 3). Notably, the rates of decrease in EGFR and ErbB2 levels were comparable, indicating that the stabilities of both are HSP90 dependent. Furthermore, both GA and AT13387 treatment

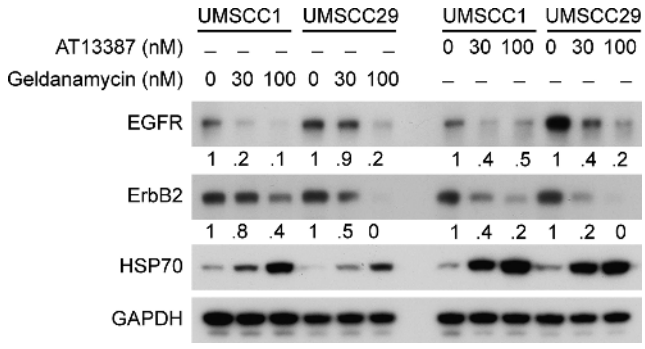

Figure 3. Effects of HSP90 inhibition on WT-EGFR and ErbB2. To assess EGFR degradation relative to ErbB2, UMSCC1, and UMSCC29B cell lines harboring WT-EGFR were treated with either GA (30 and 100 nM) or AT13387 (30 and 100 nM) for 12 hours. Immunoblot analysis was carried out to detect the effect on EGFR and ErbB2 levels. At 12 hours, loss of EGFR and ErbB2 in response to GA or AT13387 was comparable.

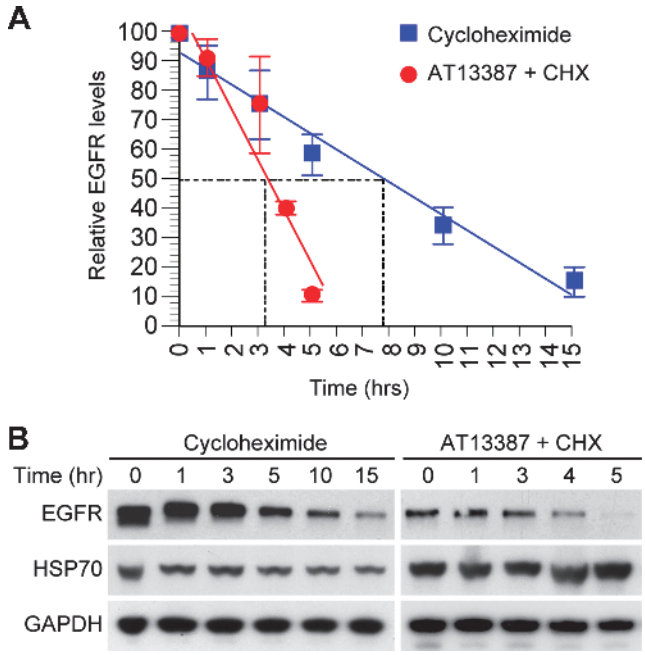

Figure 4. Effects of HSP90 inhibition on EGFR stability. To assess whether inhibition of HSP90 affects stability of EGFR, UMSCC1 cells were treated with AT13387 (30 nM) or DMSO for 12 hours, followed by CHX (100 μg/ml) to block the new protein synthesis. (A) The level of EGFR was assessed at multiple time points using immunoblot analysis, and half-life was calculated. Inhibition of HSP90 reduced the half-life of EGFR from 8 to 3.7 hours. (B) Representative blots of EGFR are shown.

led to compensatory increases in HSP70 levels, indicative of inhibition of HSP90 activity [26]. These results support that WT-EGFR is also a HSP90 client, and inhibition of HSP90 activity induces comparable degrees of EGFR and ErbB2 degradation.

If WT-EGFR were a client of HSP90, we would expect that inhibition of HSP90 activity would reduce the stability of EGFR. To analyze the effect of HSP90 inhibition on EGFR stability, UMSCC1 cells were treated with AT13387 (30 nM) for 12 hours, followed by 100 μg/ml of CHX to block new protein synthesis. The combination of AT13387 and CHX was compared with CHX alone at several time points to assess the rate of EGFR loss. The combination of AT13387 and CHX reduced the half-life of EGFR to less than 4 hours compared with 8 hours without HSP90 inhibition. These results indicate that inhibition of HSP90 activity by AT13387 accelerated the loss of EGFR (Figure 4).

In Vivo *Effects of HSP90 Inhibition on HNSCC Tumors Driven by WT-EGFR*

If the direct interaction between HSP90 and WT-EGFR were important for the tumors driven by WT-EGFR, inhibition of this interaction would be expected to slow tumor growth. Therefore, we treated UMSCC1 tumor-bearing mice with AT13387. The 3-week treatment produced significant tumor growth delay (Figure 5*A*) and prolonged survival of mice (Figure 5*B*). To see if tumor growth delay induced by AT13387 treatment had any effect on EGFR protein level, three tumors were removed 24 hours after the last AT13387 injection (day 16 from the initiation of treatment), and the relative EGFR expression was assessed by immunoblot analysis and immunostaining. Similar to our *in vitro* observations (Figure 3), we found that inhibition of

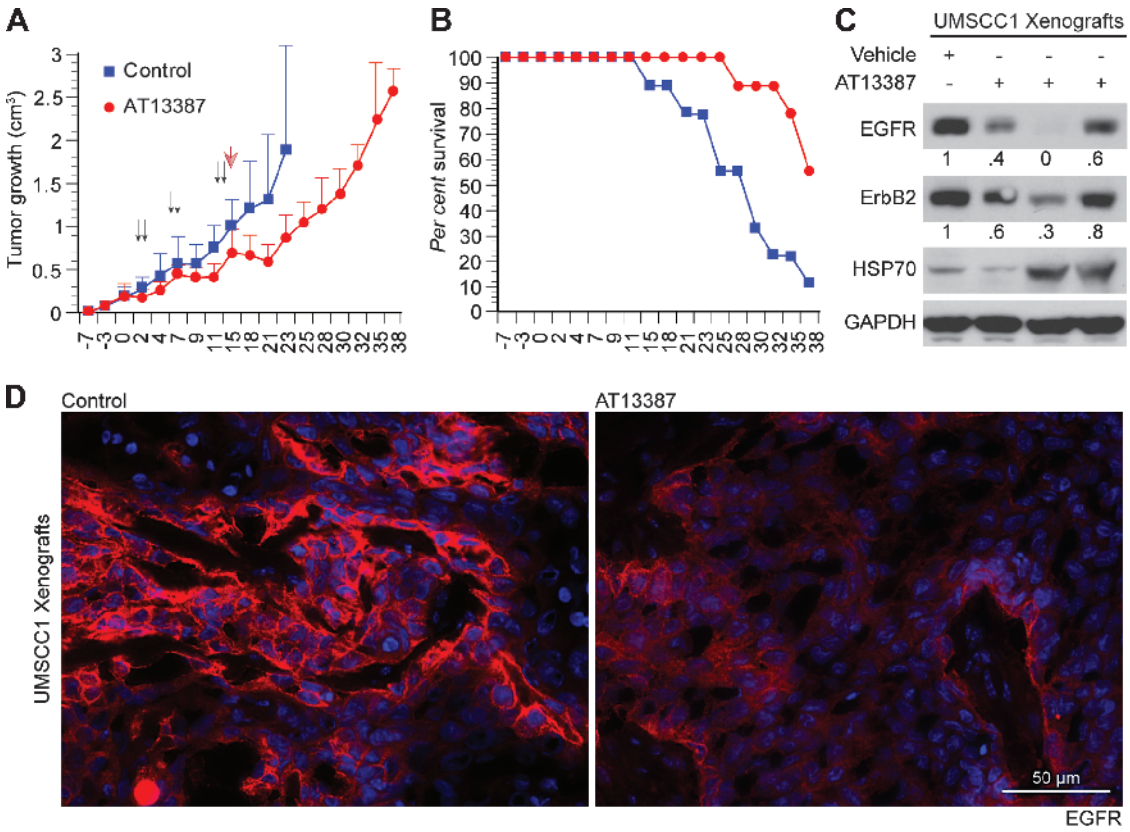

Figure 5. Effect of HSP90 inhibitor AT13387 on UMSCC1 tumor growth. (A) SCID mice were inoculated on day 0 with UMSCC1 cells and then randomized and treated on day 7. Mice received 55 mg/kg AT13387 dissolved in cyclodextrin solution or vehicle alone. Animals were treated through the intraperitoneal route on two consecutive days per week (Monday and Tuesday, indicated by the arrows), for a total of 3 weeks. Mice were euthanized when moribund beginning on day 18, as shown in B by the Kaplan-Meier plot. Student's *t* test revealed a significant difference ($P < .05$) in tumor volume between AT13387 treated and control animals during the treatment. (B) Effect of AT13387 on the survival of mice. AT13387 treatment improved the survival of UMSCC1-bearing mice. (C) Vehicle- ($n = 2$) and AT13387- ($n = 3$) treated mice were euthanized on day 16, tumors were harvested, and the effect of AT13387 on EGFR, ErbB2, and HSP70 was analyzed by immunoblot analysis. (D) Effect on EGFR expression by AT13387 was further confirmed by immunostaining.

HSP90 activity caused reduction of EGFR in UMSCC1 xenografts (Figure 5, *C* and *D*).

Discussion

In this study, we have found that mature WT-EGFR interacts with HSP90 in both tumor and normal cells. We detected this interaction using immunoadsorption of endogenous or ectopically expressed HSP90 or WT-EGFR and confirmed the direct interaction between HSP90 and EGFR by *in vitro* GST pull-down experiment. The degradation of EGFR on HSP90 inhibition is due to a decrease in the protein stability of mature EGFR, indicating that WT-EGFR stability is critically dependent on HSP90's chaperone function. The finding that HSP90 inhibition by AT13387 degrades EGFR and suppresses growth of WT-EGFR–driven HNSCC tumors underscores the biologic and potential clinical significance of these observations.

Although the major focus of research related to EGFR-targeted therapy has been development of agents to block EGFR phosphorylation [27], we and others have found that the physical presence of EGFR is critical for cell survival. Small interfering RNA, chemotherapy- or radiotherapy-induced degradation of EGFR causes cell death in EGFR-driven tumor cells [1,3,5,6,28]. Blockade of HSP90 activity is known to induce EGFR degradation in cells that harbor erlotinib-resistant T790M or the ligand-independent truncated form of EGFR (EGFRvIII) [16,17]. Overall, these results suggest that HSP90 inhibitors may have a role in overcoming erlotinib resistance.

Although it is known that HSP90 inhibitors cause overall EGFR levels to decrease over time [29], this has been attributed to an effect only on the nascent EGFR, which is a client of HSP90 [30]. More recently, the stability of mutant [15,16] and truncated forms of EGFR (EGFRvIII) was shown to be regulated by HSP90 [17]. However, only minimal interactions between mature EGFR and HSP90 have been reported [31,32], and none of these reports has indicated that WT-EGFR and HSP90 interact directly. This apparent lack of interaction was unexpected because other EGFR family members such as ErbB2 [32,33] and ErbB3 [34] are known to interact directly with HSP90, and the stability of both nascent and mutant forms of EGFR seems to depend on the HSP90 activity [17]. There are a number of possible reasons why WT-EGFR and HSP90 interaction was previously not detected. First, the studies that have investigated the interaction between nascent EGFR and HSP90 have focused on COS7 cells in an overexpression system [23,30]. It is possible that tumor cells, which tend to contain much higher levels and a more active form of HSP90, would be more likely to reveal HSP90-EGFR binding. This may also explain why only a small amount of EGFR is immunoadsorbed with HSP90 from MRC5 cells (normal fibroblasts), which express only a moderate amount of EGFR. The second, and

perhaps more likely possibility, is related to the dynamic nature of the interaction between EGFR and HSP90. At any given time, the amount of EGFR interacting with HSP90 may be minimal compared with other clients such as ErbB2, which is known to form a more stable interaction with HSP90 [31]. Our data would be consistent with this idea because stabilization of the HSP90 clients using ammonium molybdate caused the amount of EGFR immunoadsorbed with HSP90 to be enhanced several fold.

HSP90 expression in tumors is known to be elevated relative to that in normal tissue [35,36]. We also observed a high expression of HSP90 and EGFR in HNSCC patient tumor, similar to UMSCC1 xenografts (Figure 1*E*). This high expression of HSP90 in tumors most likely provides stability to many oncogenic kinases that are either overexpressed or activated through mutations. Previous studies have demonstrated that only nascent or mutated EGFR binds to HSP90 [17], but in this study using subcellular fractions, we found that not only the cytoplasmic but also the membrane-bound mature EGFR coimmunoprecipiates with HSP90 (Figure 2*A*). Treatment with HSP90 inhibitors led to a rapid loss of total EGFR (Figures 3 and 4), indicating a critical role of HSP90 in regulation of EGFR stability. These findings were confirmed by a proof-of-principle *in vivo* therapy experiment where inhibition of HSP90 activity by AT13387 treatment caused growth delay of a WT-EGFR–driven head and neck carcinoma, which correlated with a decreased expression of EGFR.

Our data confirm that blocking the chaperone function of HSP90 with HSP90 ATPase inhibitors, leading to EGFR degradation, is an attractive approach for treatment of EGFR-dependent tumors. However, given the essential proteins for which HSP90 functions as a chaperone [37], an approach targeting the specific interaction between EGFR and HSP90 could result in more selective cancer cell killing. Although we have demonstrated that mature WT-EGFR is an HSP90 client protein, the details of the interaction between EGFR and HSP90 still need to be determined. Indeed, an in-depth knowledge of HSP90 interaction with EGFR would provide an opportunity to develop an agent that would selectively disrupt EGFR-HSP90 interactions and cause EGFR degradation without affecting HSP90's other chaperone functions. The contact surface through which one EGFR family member, ErbB2, interacts with HSP90 has been shown to be in the M5 domain [32], which could be the starting point for designing a more targeted approach to disrupt the interaction between EGFR and HSP90. Studies focusing on identifying this region and developing specific methods to block the interaction between EGFR and HSP90 are currently underway in our laboratory.

Acknowledgments

The authors thank A. Helman, R. Menawat, R.V. Premkumar, and M.A. Davis for technical assistance.

References

[1] Doody JF, Wang Y, Patel SN, Joynes C, Lee SP, Gerlak J, Rolser RL, Li Y, Steiner P, Bassi R, et al. (2007). Inhibitory activity of cetuximab on epidermal growth factor receptor mutations in non–small cell lung cancers. *Mol Cancer Ther* **6**, 2642–2651.

[2] Sawai A, Chandarlapaty S, Greulich H, Gonen M, Ye Q, Arteaga CL, Sellers W, Rosen N, and Solit DB (2008). Inhibition of Hsp90 down-regulates mutant epidermal growth factor receptor (EGFR) expression and sensitizes EGFR mutant tumors to paclitaxel. *Cancer Res* **68**, 589–596.

[3] Burtness B (2005). The role of cetuximab in the treatment of squamous cell cancer of the head and neck. *Expert Opin Biol Ther* **5**, 1085–1093.

[4] Ray D, Ahsan A, Helman A, Chen G, Hegde A, Gurjar SR, Zhao L, Kiyokawa H, Beer DG, Lawrence TS, et al. (2011). Regulation of EGFR protein stability by the HECT-type ubiquitin ligase SMURF2. *Neoplasia* **13**, 570–578.

[5] Argiris A, Duffy AG, Kummar S, Simone NL, Arai Y, Kim SW, Rudy SF, Kannabiran VR, Yang X, Jang M, et al. (2011). Early tumor progression associated with enhanced EGFR signaling with bortezomib, cetuximab, and radiotherapy for head and neck cancer. *Clin Cancer Res* **17**, 5755–5764.

[6] Ahsan A, Hiniker SM, Ramanand SG, Nyati S, Hegde A, Helman A, Menawat R, Bhojani MS, Lawrence TS, and Nyati MK (2010). Role of epidermal growth factor receptor degradation in cisplatin-induced cytotoxicity in head and neck cancer. *Cancer Res* **70**, 2862–2869.

[7] Ahsan A, Hiniker SM, Davis MA, Lawrence TS, and Nyati MK (2009). Role of cell cycle in epidermal growth factor receptor inhibitor–mediated radiosensitization. *Cancer Res* **69**, 5108–5114.

[8] Feng FY, Lopez CA, Normolle DP, Varambally S, Li X, Chun PY, Davis MA, Lawrence TS, and Nyati MK (2007). Effect of epidermal growth factor receptor inhibitor class in the treatment of head and neck cancer with concurrent radiochemotherapy *in vivo*. *Clin Cancer Res* **13**, 2512–2518.

[9] Feng FY, Varambally S, Tomlins SA, Chun PY, Lopez CA, Li X, Davis MA, Chinnaiyan AM, Lawrence TS, and Nyati MK (2007). Role of epidermal growth factor receptor degradation in gemcitabine-mediated cytotoxicity. *Oncogene* **26**, 3431–3439.

[10] Levkowitz G, Waterman H, Zamir E, Kam Z, Oved S, Langdon WY, Beguinot L, Geiger B, and Yarden Y (1998). c-Cbl/Sli-1 regulates endocytic sorting and ubiquitination of the epidermal growth factor receptor. *Genes Dev* **12**, 3663–3674.

[11] Levkowitz G, Waterman H, Ettenberg SA, Katz M, Tsygankov AY, Alroy I, Lavi S, Iwai K, Reiss Y, Ciechanover A, et al. (1999). Ubiquitin ligase activity and tyrosine phosphorylation underlie suppression of growth factor signaling by c-Cbl/Sli-1. *Mol Cell* **4**, 1029–1040.

[12] Huang Y, Kim SO, Jiang J, and Frank SJ (2003). Growth hormone–induced phosphorylation of epidermal growth factor (EGF) receptor in 3T3-F442A cells. Modulation of EGF-induced trafficking and signaling. *J Biol Chem* **278**, 18902–18913.

[13] Neckers L, Mollapour M, and Tsutsumi S (2009). The complex dance of the molecular chaperone Hsp90. *Trends Biochem Sci* **34**, 223–226.

[14] Workman P (2004). Altered states: selectively drugging the Hsp90 cancer chaperone. *Trends Mol Med* **10**, 47–51.

[15] Yang S, Qu S, Perez-Tores M, Sawai A, Rosen N, Solit DB, and Arteaga CL (2006). Association with HSP90 inhibits Cbl-mediated down-regulation of mutant epidermal growth factor receptors. *Cancer Res* **66**, 6990–6997.

[16] Shimamura T, Li D, Ji H, Haringsma HJ, Liniker E, Borgman CL, Lowell AM, Minami Y, McNamara K, Perera SA, et al. (2008). Hsp90 inhibition suppresses mutant EGFR-T790M signaling and overcomes kinase inhibitor resistance. *Cancer Res* **68**, 5827–5838.

[17] Lavictoire SJ, Parolin DAE, Klimowicz AC, Kelly JF, and Lorimer IAJ (2003). Interaction of Hsp90 with the nascent form of the mutant epidermal growth factor receptor EGFRvIII. *J Biol Chem* **278**, 5292–5299.

[18] Nyati MK, Maheshwari D, Hanasoge S, Sreekumar A, Rynkiewicz SD, Chinnaiyan AM, Leopold WR, Ethier SP, and Lawrence TS (2004). Radiosensitization by pan ErbB inhibitor CI-1033 *in vitro* and *in vivo*. *Clin Cancer Res* **10**, 691–700.

[19] Graham B, Curry J, Smyth T, Fazal L, Feltell R, Harada I, Coyle J, Williams B, Reule M, Angove H, et al. (2012). The heat shock protein 90 inhibitor, AT13387, displays a long duration of action *in vitro* and *in vivo* in non–small cell lung cancer. *Cancer Sci* **103**, 522–527.

[20] Woodhead AJ, Angove H, Carr MG, Chessari G, Congreve M, Coyle JE, Cosme J, Graham B, Day PJ, Downham R, et al. (2010). Discovery of (2,4-dihydroxy-5-isopropylphenyl)-[5-(4-methylpiperazin-1-ylmethyl)-1,3-dihydroisoindol-2-yl]methanone (AT13387), a novel inhibitor of the molecular chaperone Hsp90 by fragment based drug design. *J Med Chem* **53**, 5956–5969.

[21] Xu WP, Mimnaugh E, Rosser MFN, Nicchitta C, Marcu M, Yarden Y, and Neckers L (2001). Sensitivity of mature ErbB2 to geldanamycin is conferred by its kinase domain and is mediated by the chaperone protein Hsp90. *J Biol Chem* **276**, 3702–3708.

[22] Pratt WB and Toft DO (1997). Steroid receptor interactions with heat shock protein and immunophilin chaperones. *Endocr Rev* **18**, 306–360.

[23] Xu WP, Yuan XT, Xiang ZX, Mimnaugh E, Marcu M, and Neckers L (2005). Surface charge and hydrophobicity determine ErbB2 binding to the Hsp90 chaperone complex. *Nat Struct Mol Biol* **12**, 120–126.

[24] Wada T, Qian XL, and Greene MI (1990). Intermolecular association of the p185neu protein and EGF receptor modulates EGF receptor function. *Cell* **61**, 1339–1347.

[25] Citri A, Kochupurakkal BS, and Yarden Y (2004). The Achilles heel of ErbB-2/HER2—regulation by the Hsp90 chaperone machine and potential for pharmacological intervention. *Cell Cycle* **3**, 51–60.

[26] Sittler A, Lurz R, Lueder G, Priller J, Hayer-Hartl MK, Hartl FU, Lehrach H, and Wanker EE (2001). Geldanamycin activates a heat shock response and inhibits huntingtin aggregation in a cell culture model of Huntington's disease. *Hum Mol Genet* **10**, 1307–1315.

[27] Modjtahedi H and Essapen S (2009). Epidermal growth factor receptor inhibitors in cancer treatment: advances, challenges and opportunities. *Anticancer Drugs* **20**, 851–855.

[28] Weihua Z, Tsan R, Huang WC, Wu Q, Chiu CH, Fidler IJ, and Hung MC (2008). Survival of cancer cells is maintained by EGFR independent of its kinase activity. *Cancer Cell* **13**, 385–393.

[29] Sakagami M, Morrison P, and Welch WJ (1999). Benzoquinoid ansamycins (herbimycin A and geldanamycin) interfere with the maturation of growth factor receptor tyrosine kinases. *Cell Stress Chaperones* **4**, 19–28.

[30] Citri A, Harari D, Shohat G, Ramakrishnan P, Gan J, Lavi S, Eisenstein M, Kimchi A, Wallach D, Pietrokovski S, et al. (2006). Hsp90 recognizes a common surface on client kinases. *J Biol Chem* **281**, 14361–14369.

[31] Pratt WB, Morishima Y, and Osawa Y (2008). The Hsp90 chaperone machinery regulates signaling by modulating ligand binding clefts. *J Biol Chem* **283**, 22885–22889.

[32] Citri A, Gan J, Mosesson Y, Vereb G, Szollosi J, and Yarden Y (2004). Hsp90 restrains ErbB-2/HER2 signalling by limiting heterodimer formation. *EMBO Rep* **5**, 1165–1170.

[33] Sidera K, Gaitanou M, Stellas D, Matsas R, and Patsavoudi E (2008). A critical role for HSP90 in cancer cell invasion involves interaction with the extracellular domain of HER-2. *J Biol Chem* **283**, 2031–2041.

[34] Dote H, Cerna D, Burgan WE, Camphausen K, and Tofilon PJ (2005). ErbB3 expression predicts tumor cell radiosensitization induced by Hsp90 inhibition. *Cancer Res* **65**, 6967–6975.

[35] Neckers L and Workman P (2012). Hsp90 molecular chaperone inhibitors: are we there yet? *Clin Cancer Res* **18**, 64–76.

[36] Ferrarini M, Heltai S, Zocchi MR, and Rugarli C (1992). Unusual expression and localization of heat-shock proteins in human tumor-cells. *Int J Cancer* **51**, 613–619.

[37] Trepel J, Mollapour M, Giaccone G, and Neckers L (2010). Targeting the dynamic HSP90 complex in cancer. *Nat Rev Cancer* **10**, 537–549.

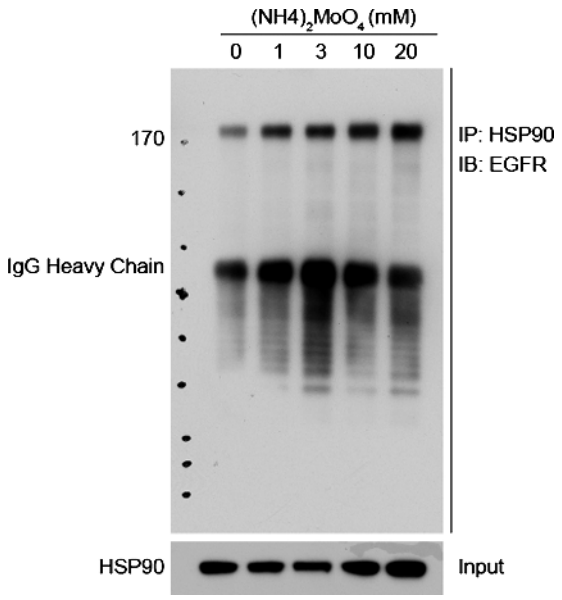

Figure W1. Effect of ammonium molybdate on the interaction of mature WT-EGFR with HSP90. The effect of ammonium molybdate on the interaction between WT-EGFR and HSP90 was assessed by IP as shown in Figure 1*A*. The full-length immunoblot shows an increase in the interaction between mature EGFR (~170 kDa) with HSP90 with increasing concentrations of ammonium molybdate.

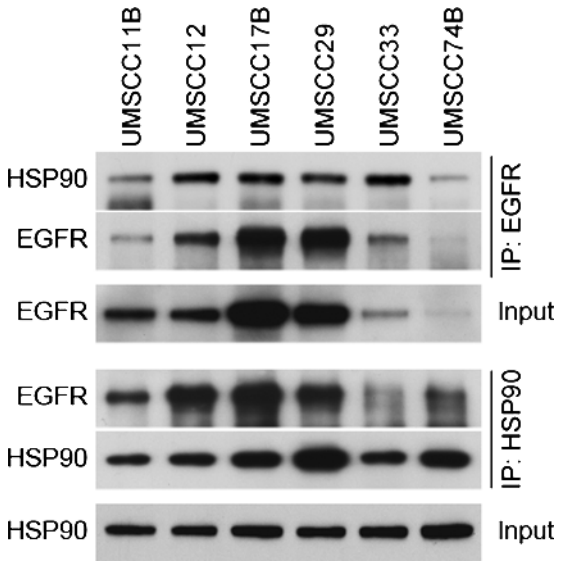

Figure W2. Specificity of immunoadsorption of EGFR and HSP90. The specificity of antibody and the interaction between EGFR and HSP90 were confirmed by IP of EGFR or HSP90 followed by immunoblot analysis of HSP90 or EGFR, in six HNSCC cell lines. Both approaches yielded relatively similar results, indicating the specificity of protein-protein interaction.